

# Research Journal of Pharmaceutical, Biological and Chemical Sciences

## Hydroxyapatite Formation and Bone Bonding Ability of Ternary Borate Glasses Ceramics Containing ZnO.

AM Abdelghany<sup>\*1</sup>, Nadia H Elsayed<sup>2,3</sup>, and Asma M ALturki<sup>3,4</sup>.

<sup>1</sup>Spectroscopy Dept., Physics Division, National Research Center, 12311, Cairo, Egypt.

<sup>2</sup>Department of Polymers and Pigments, National Research Center, Dokki, Cairo 12311, Egypt.

<sup>3</sup>Department of Chemistry, Faculty of Science, University of Tabuk, Tabuk 71421, Saudi Arabia.

<sup>4</sup>University of Dammam College of Education in Jubail, Assistance Subjects Department.

### ABSTRACT

Ternary soda lime borate glass ceramics and samples of the same nominal composition containing ZnO were prepared via two step nucleation and crystallization regime. Prepared samples studied for their bone bonding ability. Fourier transform infrared (FTIR) absorption spectra measurements were carried out for the prepared glasses before and after immersion in simulated body fluid (SBF) for one or two weeks to justify the appearance of calcium phosphate (hydroxyapatite (HA)) which is an indication for bone bonding ability. X-ray diffraction (XRD) patterns were measured for prepared samples before and after immersion in SBF for two weeks. XRD measurements confirm the appearance of HA which showed distinction with ZnO content. The overall data are explained on the basis of current views about the corrosion behavior of borate glasses including hydrolysis and direct dissolution mechanism.

**Keywords:** Borate bioglass; ZnO; SBF; FTIR ; XRD

*\*Corresponding author*

## INTRODUCTION

In recent years, many authors has focused on the development of new materials that stimulate a biochemical response from living tissue in order to obtain a strong chemical bond with biological fixation between the prosthesis and the tissue [1, 2]. Bioactive modified soda lime silica glass 45S5 (Bioglass<sup>®</sup>) is the oldest bioactive material, first reported by Hench et al. in 1971 [3] and is now a very well-characterized material that has found use in a number of biomedical applications such as orthopaedic implant and bone filling material [4].

Hench was the first to develop bioactive glasses and these glasses were able to bond to tissues [5]. Various studies were performed to ensure that bioactive glasses are safe for clinical applications. Wilson et al reviewed [6] these studies and proposed that bioactive glasses are safe for clinical use.

Borate bioactive glass has been shown to convert faster and more completely to hydroxyapatite and enhance new bone formation in vivo when compared to silicate bioactive glass (such as 45S5 and 13-93 bioactive glass). Borate based bioactive glasses have been studied for several in-vivo applications including, bone replacement, a treatment for osteoarthritis, and drug delivery systems [7]. Richard [8] implanted particles of a 45S5 borate analog (complete exchange of boron for silica) in rat femurs and the glass converted to hydroxyapatite at a significantly accelerated rate and bone grew in and attached to the glass particles.

Bioactivity or bone-bonding ability has been also shown to be dependent on the chemical composition and structure of bioactive glass [9, 10]. In order to reach acceptable and improved bioactivity, several oxides such as MgO, ZnO, SrO have been suggested and investigated into various bioactive glasses [11-14].

Zinc ions have been known to encourage attachment, proliferation of osteoblast and inhibit osteoclastic cell [15]. Moreover, zinc may serve as cofactor for many enzymes, stimulate for protein synthesis, responsible for DNA replication [16] and also involved in calcification mechanism [17]. It also inhibits the transformation of amorphous apatite into crystalline carbonated hydroxyapatite [18]. It is assumed that bioactive glass with high Zn content showed no apatite formation even after 60 days of immersion in SBF [19].

The aim of the present work is to study the effect of ZnO additions up to 10% replacing CaO on the bioactivity of ternary soda lime borate glass ceramics using FTIR absorption spectral measurements, X-ray diffraction (XRD) and scanning electron microscopy (SEM) after immersion in simulated body fluid (SBF) for different time intervals at 37°C.

## EXPERIMENTAL

### Preparation of the Glasses

Accurately weighed batches were transformed to glasses by conventional melting and annealing technique. The raw materials include pure chemicals of orthoboric acid ( $H_3BO_3$ ) for  $B_2O_3$ , soda and lime were added in the form of their respective heavy carbonates. Zinc oxide was introduced as such. Melting was carried out in platinum crucibles in SiC heated furnace at 1100°C for 2 hours. The crucibles were rotated at intervals to promote homogeneity to the melts. Then the melts were cast in preheated stainless steel molds to the appropriate dimensions. The glassy samples were immediately transferred to a muffle furnace regulated at 400°C for annealing. The muffle after 1 hour was switched off and left to cool to room temperature at a rate of 30°C/hour. Table (1) depicts the chemical composition of the studied glasses.

Table 1: Chemical composition of studied glasses

Glass No.	Na <sub>2</sub> O	CaO	B <sub>2</sub> O <sub>3</sub>	ZnO
Zn1	15	25	60	0
Zn2	15	23	60	2
Zn3	15	20	60	5
Zn4	15	10	60	10

### Differential thermal analysis measurements (DTA)

DTA measurements were carried on powdered samples, which were examined up to 1000°C using a powdered alumina as a reference. The heating rate was 10°C/minute. The DTA data were used to obtain the proper heat treatment temperatures in order to be able to obtain the corresponding glass-ceramic derivatives. Briefly, these DTA data represent the glass transition temperatures and the onset of crystallization temperatures (nucleation 475°C/6h and crystal growth 650 °C/12 h) for each studied composition.

### Heat-treatment Regime (Conversion to Glass-Ceramic)

The parent glasses were thermally heat treated in two-step regime at the temperatures mentioned before (475, 650 °C). Each glass was slowly heated (5°C/min) to the first nucleation temperature (475°C) for the formation of sufficient nuclei sites and after holding for the specified time (6h), was then further heated to reach the second chosen crystal growth temperature (650 °C). After a second hold (6h) at the second temperature to have full crystal growth process, the furnace was left to cool to room temperature at a rate of 30°C/h. (note that the letters GC was added before glass name to indicate glass ceramic).

### X-ray diffraction measurements (XRD)

The heat treated glass-ceramic derivatives were analyzed by an X-ray diffraction technique to identify the crystalline phases that were precipitated during the heat-treatment process. The heat-treated samples were grounded and the fine powder was examined using a Philips diffractometer (pw 1390) adopting a Ni-filter and a Cu-target. It should be mentioned that X-ray diffraction investigations were also carried out for the glasses before and after immersion in SBF for a period up to two weeks and also for the glass-ceramic samples before and after immersion for the same period.

### Structural analysis of bioactivity using FTIR absorption spectroscopy

FT infrared absorption spectral measurements of the glasses were carried out through the KBr disc technique. The measurements were done at room temperature (~20°C) in the wavenumber range of 4000-400 cm<sup>-1</sup> using a Fourier transform IR spectrometer (Nicolet i10). Fine powders of the glasses were mixed with KBr powder in the ratio 1:100 and the mixtures were subjected to a load of 5 tons/cm<sup>2</sup> in an evocable die to produce clear homogeneous discs. Then the IR spectra were immediately taken after preparing the discs to avoid moisture effect.

The measurements were repeated after each immersion of the fine powders in simulated body fluid for prolonged times (1, 2 weeks).

### Structural analysis using scanning electron microscopy

Scanning electron microscopic [SEM] investigations were carried out on glass-ceramic derivatives before and after immersion in SBF for prolonged times. This study was performed using an SEM Model Philips XL 30, attached with EDX unit, accelerating voltage 30 kV, magnification 10X up to 400,000. All samples were coated with gold for morphological investigations.

### Solubility testing

The solubility of the studied borate glasses was determined by measuring the weight loss after immersion in SBF at human body temperature (37 °C). Samples were polished and refined with 600 grit polishing papers. The sample dimensions were measured accurately and washed in acetone for few minutes and then the sample was placed in a polyethylene beaker containing pre-calculated volume of SBF (ratio between geometric area of the glass sample and volume of the solution was fixed as 0.075 cm<sup>-1</sup> in all cases for comparison and to avoid defects resulting from volumetric or supersaturation differences [20]. Samples were removed and excess moisture was removed by tissue paper at various time intervals and then reweighed. After immersion, the materials started to dissolve and the same was registered for every 24 h, until the end of 480 h. By knowing the initial weight ( $M_0$ ) of each sample and the weight loss ( $M_t$ ) at time  $t$ , the % of weight loss per unit area was obtained as:

$$\% \text{ of weight loss} = \frac{M_0 - M_t}{A} \times 100 \quad (3)$$

where A is the surface area in cm<sup>2</sup>.

A regression method used for data fitting and dissolution rates in g m<sup>-2</sup>h<sup>-1</sup> was calculated according to the formula:

$$D_{\text{rate}} = (\text{slope} \times M_0 / A) \quad (4)$$

Where D<sub>rate</sub> is the dissolution rates, M<sub>0</sub> is the initial weight and A is the surface area in cm<sup>2</sup>

### pH measurements

The pH changes for the attacking leaching solution after intervals were measured using a pH meter (pH 3L5i Germany). The measurements were conducted up to 480 h for the leaching solution at a time interval of 24 h for solubility studies. The percentage of error in the measurement of pH is ±0.005 and calibration of the electrode against buffer solution was performed every 12h. The same procedure was adopted by some authors [21, 22]

## RESULTS AND DISCUSSION

### Infrared absorption spectra of crystalline glass ceramic derivatives samples before immersion

Figure (1) illustrates the FTIR spectra of glass-ceramic samples before immersion. The spectral data show that overall absorption bands within the mid region from 400 to 1650 cm<sup>-1</sup> reveal obvious splitted sharp peaks for all the studied heat-treated samples and first broad band is shifted and lies within the range from 1150-1550 cm<sup>-1</sup>.

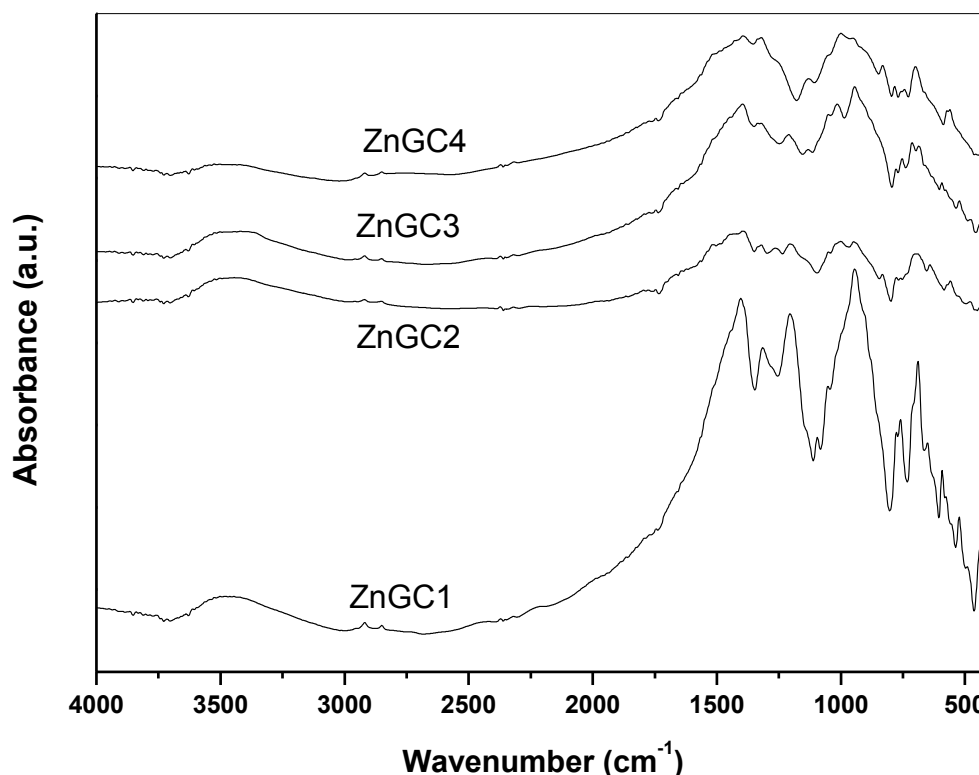


Figure 1: FTIR absorption spectra of the studied glass-ceramics before immersion in SBF.

**Infrared absorption spectra of glass-ceramics after immersion in SBF**

Figures (2 and 3) reveal the FTIR spectra of the glass-ceramic samples after immersion for one or two weeks. It is obvious that the IR spectra in the two figures show almost the same spectral characteristics which indicate the splitting of the bands within the range from 400 to 1550  $\text{cm}^{-1}$  to numerous sharp peaks together with the increase of the intensity of the near IR broad band at 3460  $\text{cm}^{-1}$ .

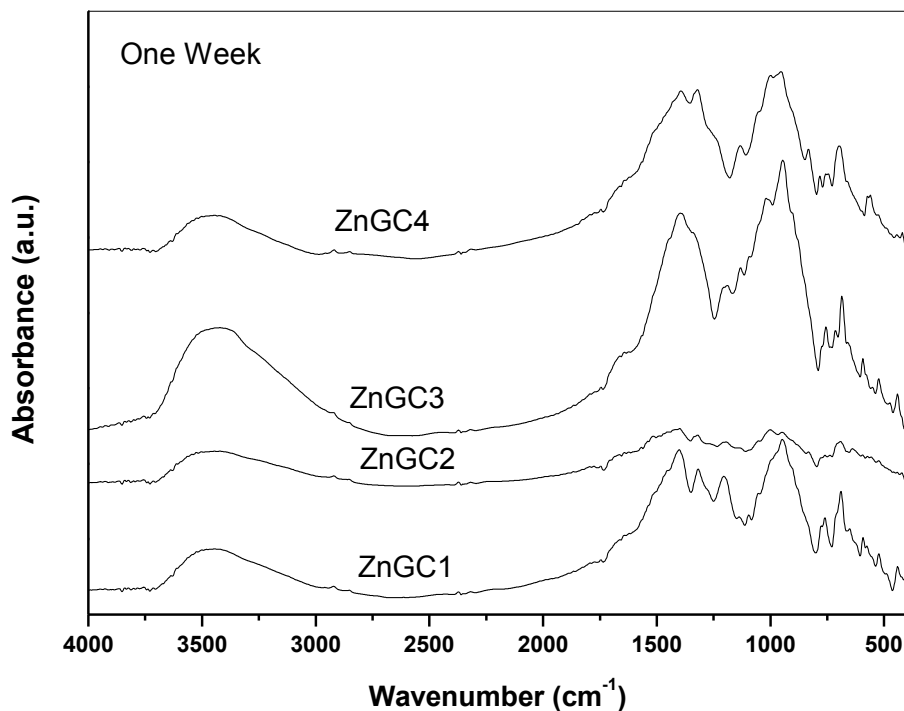


Figure 2: FTIR absorption spectra of the glass-ceramics after immersion in SBF for one week.

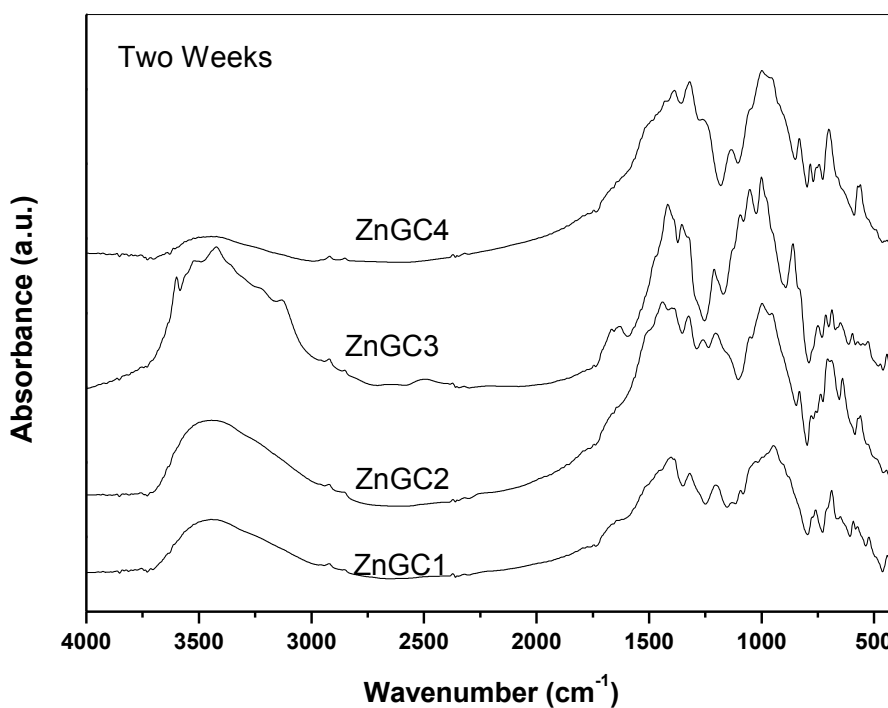


Figure 3: FTIR absorption spectra of the glass-ceramics after immersion in SBF for two week.

**pH and weight loss measurements**

Figure 4 shows the changes in pH values of the simulated body fluid at different time intervals after the glassy powder has been soaked in it. The graph shows that the pH values of solution start from value of 7.2 and reaches a constant value that depends on the different type of additive oxide.

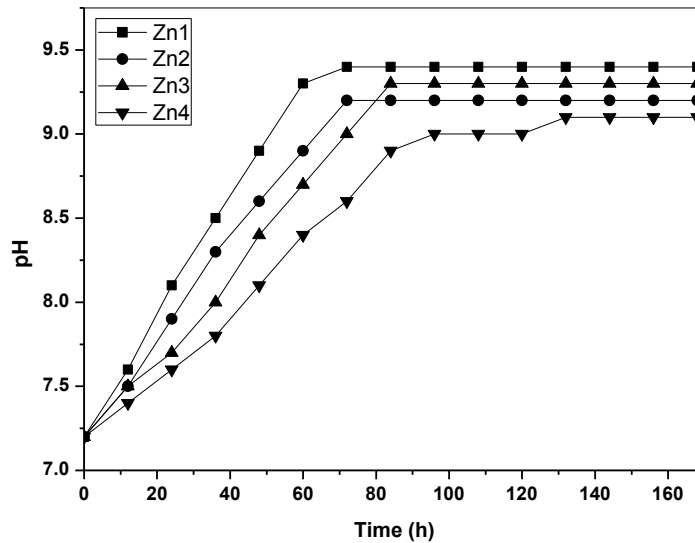


Figure 4: Changes in pH values of the simulated body fluid at different time intervals

Figure 5 shows the percentage weight losses of all prepared samples soaked in simulated body fluid solution at 37 °C as a function of time. The obtained data reveal that dissolution of samples occurs as indicated by the weight loss. The dissolution process is an important stage during both in vivo and in vitro reaction. The dissolution rate is affected by several factors including the reaction product and also the stability of the bioglass during the in vivo reaction. As it was reported that biodegradation of a material in vitro is a very complex process. Additionally it is well documented the dissolution and reaction of Ca from bioglass and P from immersion solution [1], which explains the gradually increase of the surface composition of Ca and P in all specimens.

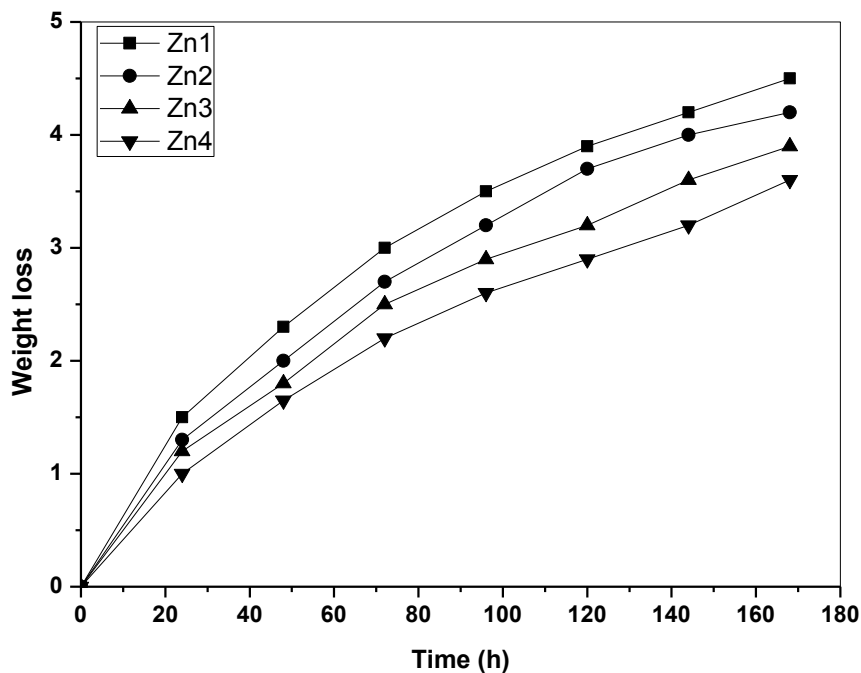


Figure 5: Weight losses of glass samples soaked in simulated body fluid solution at 37 °C as a function of time

The results obtained in (Fig. 5) show a relation between the percent weight loss versus the time of immersion in simulated body fluid. It is noticed that the percent weight loss in the glassy samples containing higher content of ZnO is greater than that of the rest of bioglasses containing lower contents.

The experimental data were plotted again after using a semiempirical equation from which one can use for the calculation of normalized i-th element dissolution rate, this equation is given by:-

$$NR_i = \beta_i \exp\left(-\frac{t}{\tau_i}\right) + W_i \left(1 - \exp\left(-\frac{t}{\tau_i}\right)\right) \tag{1}$$

where  $\beta_i$  is the i-th component initial dissolution rate,  $W_i$  is the i-th component final dissolution rate, and  $\tau_i$  is i-th component time constant. Glass dissolution is identical if  $W_i$  has the same value for each component of our prepared glasses.

An integration of the previous semiempirical equation (1) yields:

$$NL_i = \tau_i(\beta_i - W_i) \left[1 - \exp\left(-\frac{t}{\tau_i}\right)\right] + W_i t \tag{2}$$

Where  $NL_i$  is the normalized i-th element mass release.

A graphical representation of the parameter  $\beta_i$  (tangent of the first linear portion of curve of dissolution),  $W_i$  (tangent of the second linear portion of curve of dissolution) and  $\tau_i$  is given in figure 6. From this graph, one can be able to determine the **transition time** which means that the time needed for conversion from the initial stage to the final stage of dissolution, and expressed and estimated as  $3\tau_i$

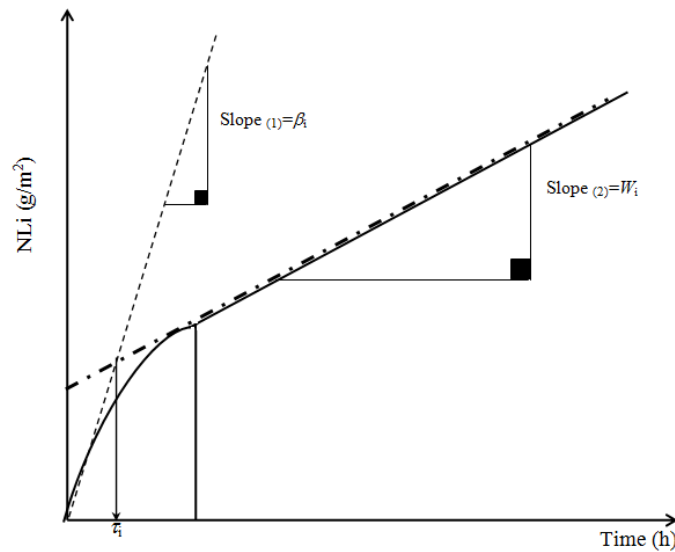


Figure 6: A graphical representation of the parameter  $\beta_i$ ,  $W_i$  and  $\tau_i$

From figure 5, the parameters  $\beta_i$ ,  $W_i$  and  $\tau_i$  are calculated. These parameters are then used to calculate the normalized i-th element dissolution rate ( $NR_i$ ) and normalized i-th element mass release ( $NL_i$ ). One can note that our calculated values for  $\tau_i$  are nearly the same for each type of additives fluoride and equal to  $\approx 0.013$ .

A plot of normalized i-th element dissolution rate ( $NR_i$ ) and time is given in figure 7. A plot of normalized i-th element mass release ( $NL_i$ ) and time is given in figure 8. Time dependence  $NR_i(t)$  indicates also identical dissolution, which occurs when the  $NR_i(t)$  values for each element are equal.

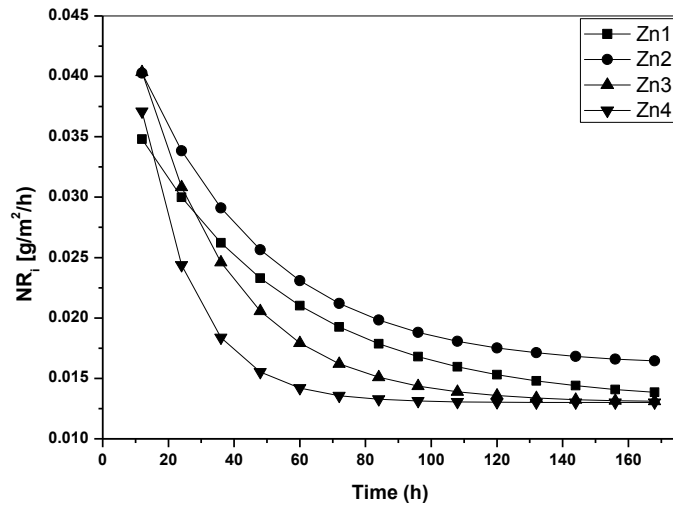


Figure 7: Plot of normalized i-th element dissolution rate ( $NR_i$ ) and time

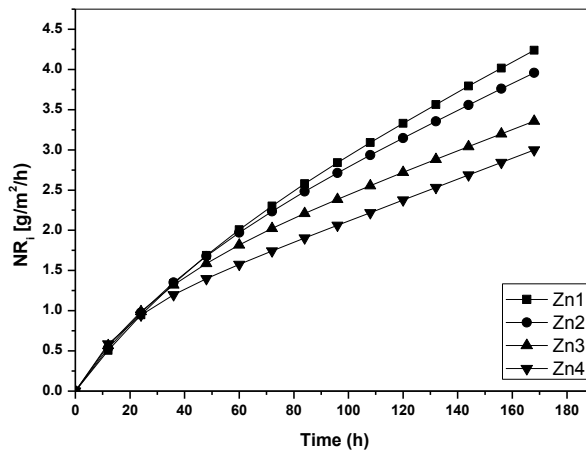
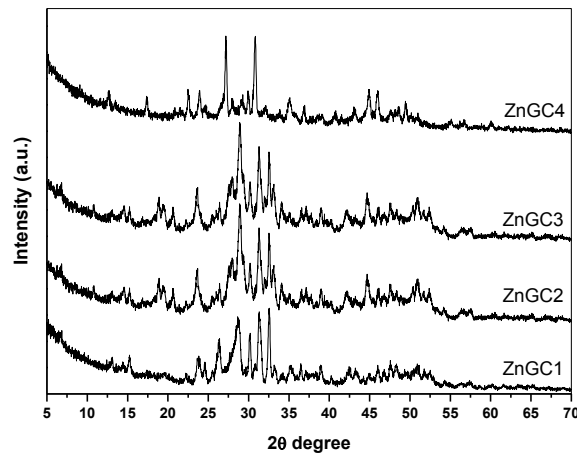


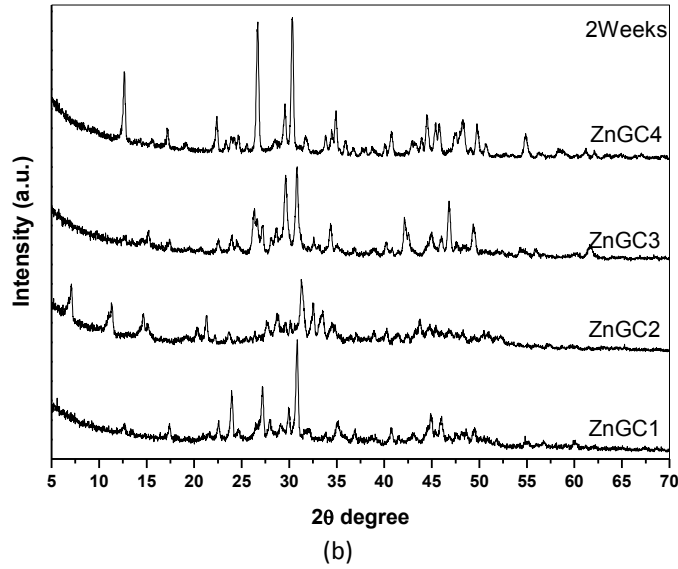
Figure 8: Plot of normalized i-th element mass release ( $NL_i$ ) and time

**XRD**

Figure (9-a) illustrates the X-ray diffraction patterns of the glass-ceramic samples before immersion. The crystalline phases identified are of crystalline calcium sodium borates and calcium borates. Upon immersion of the glass-ceramic samples for two weeks, the calcium borate phases are identified beside crystalline hydroxyapatite phase and this last HA phase increases in intensity with ZnO content as shown in fig (9-b).



(a)

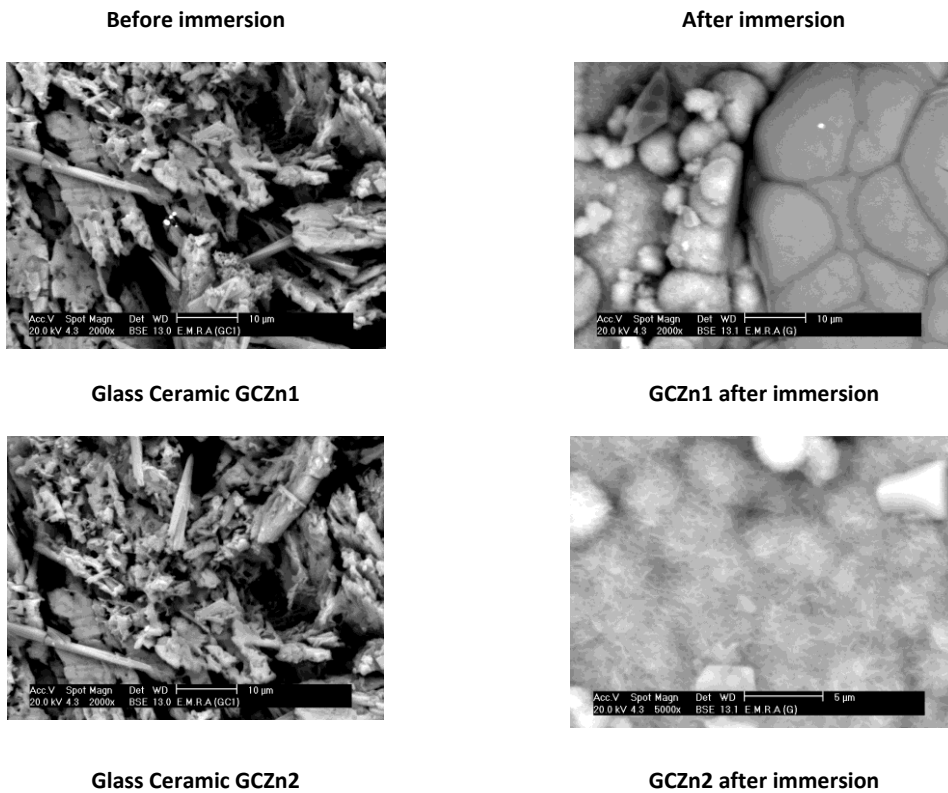


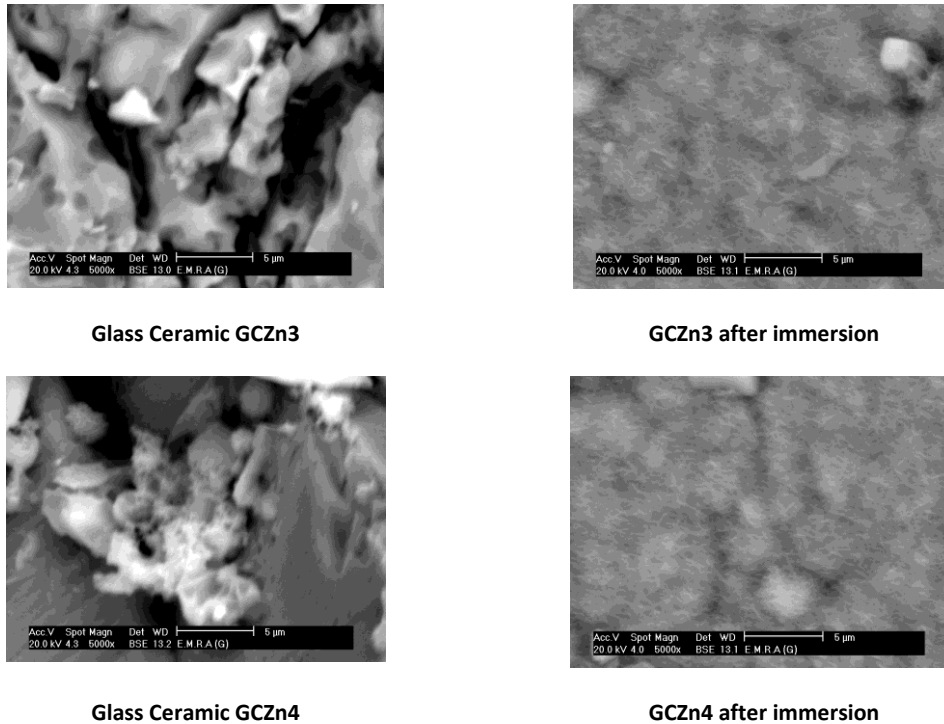
(a) Before and (b) after immersion in SBF for two week.

Figure 9: X-ray diffraction of the glass-ceramics

SEM

Figure (10) illustrates the SEM micrographs of the glass ceramics before and after immersion in SBF. The images before immersion reveal crystalline structure with increase in size of microcrystals with increasing ZnO content while after immersion, the glass ceramics SEM micrograph shows cotton like structure indicating the appearance of crystalline phase identified to be calcium phosphate hydrpoxo apatite layer by XRD.





**Figure 10: SEM images for the prepared glass-ceramics before (Left) and after immersion in SBF for two weeks (right).**

### CONCLUSION

Soda lime borate glasses containing up to 10% ZnO substituting CaO were prepared and converted to their corresponding glass ceramic derivative through heat treatment regime. Prepared glass ceramics was characterized for their bone bonding ability after immersion in SBF up to two weeks. Appearance of the FTIR spectral band within the wavenumber range ( $530-650\text{ cm}^{-1}$ ) indicating the formation of hydroxyapatite layer at the surface.

XRD of the glass-ceramic before immersion shows a crystalline crystalline calcium sodium borates and calcium borates in addition to crystalline hydroxyapatite phase after immersion which increases with increasing ZnO content.

SEM investigations of the prepared glasses ceramics show the morphological features of micro-crystalline calcium sodium borate and calcium borate before immersion. While, rounded crystalline features of hydroxyapatite are identified and increases with the ZnO content after immersion.

### ACKNOWLEDGEMENT

The authors would like to acknowledge financial support for this work, from the Deanship of Scientific Research (DSR), University of Tabuk, Tabuk, Saudi Arabia, under grant no. S-1435-0036

### REFERENCES

- [1] W Liang, MN Rahaman, DE Day, NW Marion, GC Riley, JJ Mao. *J Non-Cryst Solids* 2008;354:1690-1696.
- [2] CR Mariappan, DM Yunos, AR Boccaccini, B Roling. *Acta Biomaterilia* 2009;5(4):1274-1283.
- [3] LL Hench, RJ Splinter, WC Allen, TK Greenlee. *J Biomed Mater Res* 1972;5(6):117-141.
- [4] W Cao, LL Hench. *Ceramics Inter* 1996;22(6):493-507.
- [5] LL Hench. *J Mater Sci Mater Med* 2006;17:967-978.
- [6] J Wilson, G Piggot, F Shoen, LL Hench. *J Biomed Mat Res* 1981;15:805-817.
- [7] MN Rahaman, DE Day, BS Bal, Q Fu, SB Jung, LF Bonewald, AP Tomsia, *Acta Biomater* 2011;7(6):2355-2373.
- [8] M Richard, *Bioactive behavior of a borate glass*, Rolla: University of Missouri Rolla, 2000.

- [9] RG Hill, DS Brauer. *J Non-Cryst Solids* 2011;357:3884-3887.
- [10] AM Abdelghany, HA ElBatal, FM EzzELDin. *Ceram Int* 2012;38:1105.
- [11] J Ma, CZ Chen, DG Wang, JH Fu. *Ceram Int* 2011;37:2377-2382.
- [12] AM AlKady, AF Ali. *Ceram Int* 2012;38:1195-1204.
- [13] X Wang, X Li, A Ito, Y Sogo. *Acta Biomater* 2011;7:3638-3644.
- [14] M Yamaguchi, H Oishi, Y Suketa. *Biochem. Pharmacol* 1987;36:4007-4012.
- [15] YF Goh, AZ Alshemary, M Akram, MR Abdul Kadir, R Hussain. *Mater Chem Phy* 2013;137(3):1031-1038.
- [16] M Yamaguchi, K Inamoto, Y Suketa. *Res Exp Med* 1986;186(5):337-342.
- [17] RL Du, J Chang. *J Inorg Mater* 2004 ;19(6) :1353-1358.
- [18] JR Jaroch, DC Clupper. *J Biomed Mater Res A* 2007;82:575-588.
- [19] G Lusvardi, G Malavasi, L Menabue, MC Menziani. *J Phys Chem B* 2002;106:9753-9760.
- [20] M Vallet-Regi, CV Ragel, AJ Salinas. *Eur J Inorg Chem* 2003;6:1029-1042.
- [21] KS Manupriya, K Thind, V Singh, G Kumar, DP Sharma, A Singh. *J Phys Chem Solids* 2009;70:1137-1141.
- [22] AM Abdelghany, H Kamal. *Ceram Int* 2014;40(6):8003-8011.